Molecular Microbiology (2015) 97(6), 1195–1208 ■
doi:10.1111/mmi.13098
First published online 17 July 2015

Bacillus subtilis SalA is a phosphorylation-dependent transcription regulator that represses *scoC* and activates the production of the exoprotease AprE

Abderahmane Derouiche,[1] Lei Shi,[1] Vladimir Bidnenko,[2] Magali Ventroux,[2] Nathalie Pigonneau,[2] Mirita Franz-Wachtel,[3] Aida Kalantari,[1] Sylvie Nessler,[4] Marie-Françoise Noirot-Gros[2] and Ivan Mijakovic[1]*

[1]*Systems and Synthetic Biology, Department of Biology and Biological Engineering, Chalmers University of Technology, Gothenburg 41296, Sweden.*
[2]*Micalis UMR1319, Institut National de la Recherche Agronomique, Jouy-en-Josas 78350, France.*
[3]*Proteome Center Tübingen, University of Tübingen, Tübingen 72076, Germany.*
[4]*Institut de Biochimie et Biophysique Moléculaire et Cellulaire, University Paris-Sud, Orsay 91405, France.*

Summary

Bacillus subtilis **Mrp family protein SalA has been shown to indirectly promote the production of the exoprotease AprE by inhibiting the expression of *scoC*, which codes for a repressor of *aprE*. The exact mechanism by which SalA influences *scoC* expression has not been clarified previously. We demonstrate that SalA possesses a DNA-binding domain (residues 1–60), which binds to the promoter region of *scoC*. The binding of SalA to its target DNA depends on the presence of ATP and is stimulated by phosphorylation of SalA at tyrosine 327. The *B. subtilis* protein-tyrosine kinase PtkA interacts specifically with the C-terminal domain of SalA *in vivo* and *in vitro* and is responsible for activating its DNA binding via phosphorylation of tyrosine 327. *In vivo*, a mutant mimicking phosphorylation of SalA (SalA Y327E) exhibited a strong repression of *scoC* and consequently overproduction of AprE. By contrast, the non-phosphorylatable SalA Y327F and the Δ*ptkA* exhibited the opposite effect, stronger expression of *scoC* and lower production of the exoprotease. Interestingly, both SalA and PtkA contain the same ATP-binding Walker domain and have thus presumably arisen from the common ancestral protein. Their regulatory interplay seems to be conserved in other bacteria.**

Accepted 18 June, 2015. *For correspondence. E-mail ivan.mijakovic@chalmers.se; Tel. +46709828446; Fax +46317723801.

Introduction

Ubiquitous ATPases of the Mrp family have been detected in bacteria and eukarya (Dardel *et al.*, 1991; Vitale *et al.*, 1996). Their defining feature is an ATP-binding domain known as the Walker motif (Walker *et al.*, 1982). Mrp proteins have a modular structure. They can possess different additional domains, and thus participate in various cellular functions. A prominent representative of eukaryal Mrp ATPases is the yeast Nbp35, which carries a Fe/S cluster at its N terminus, and is essential for the iron-sulfur protein assembly (Hausmann *et al.*, 2005). In bacteria, much less is known about the function of Mrp proteins. The *Bacillus subtilis* Mrp ATPase SalA has been described as a positive regulator of the exoprotease AprE (Ogura *et al.*, 2004). The activation of *aprE* expression by SalA is indirect. SalA inhibits the transcription of *scoC*, which codes for a repressor of *aprE* (Ogura *et al.*, 2004). The mechanism of SalA repression of *scoC* has not been clarified. Ogura *et al.* (2004) detected no canonical DNA-binding motif in the SalA sequence, and thus speculated that SalA effect may be indirect, via binding of some transcription factor or the RNA polymerase itself. In evolutionary terms, the ATP-binding domain of the bacterial Mrp proteins is very closely related to cell division ATPases of the MinD family (de Boer *et al.*, 1991) and bacterial protein-tyrosine kinases (BY-kinases) (Grangeasse *et al.*, 2012). Based on extensive sequence homology, it has been suggested that bacterial Mrp proteins, MinD proteins and BY-kinases have arisen through duplication and divergent evolution of the ancestral Walker-type ATPase (Grangeasse *et al.*, 2012).

BY-kinase genes are present in about one third of sequenced bacterial genomes (Shi *et al.*, 2014a). These bacterial kinases have been shown to phosphorylate endogenous protein substrates and regulate various cellular functions via substrate phosphorylation. Known physiological roles of BY-kinases have been extensively reviewed (Shi *et al.*, 2010; Chao *et al.*, 2014). One defining feature of BY-kinase genes seems to be their faster than

average accumulation of non-synonymous substitutions (Shi *et al*., 2014a) and the related capacity of BY-kinases to phosphorylate multiple substrates (relaxed specificity). A well-known example of a promiscuous BY-kinase is the *B. subtilis* PtkA. PtkA phosphorylates UDP-glucose dehydrogenases (Mijakovic *et al*., 2003; Petranovic *et al*., 2009), single-stranded DNA-binding proteins (Mijakovic *et al*., 2006), transcription factors (Derouiche *et al*., 2013), the division protein DivIVA (Shi *et al*., 2014b) and is involved in regulating the cell cycle (Petranovic *et al*., 2007), protein localization (Jers *et al*., 2010) and biofilm formation (Kiley and Stanley-Wall, 2010; Gerwig *et al*., 2014). *B. subtilis* PtkA must interact with its transmembrane activator, TkmA, in order to phosphorylate substrates (Mijakovic *et al*., 2003). Protein-tyrosine phosphorylation, catalysed by PtkA homologues in other bacteria, is known to control very diverse physiological processes, including exopolysaccharide synthesis (Grangeasse *et al*., 2003; Minic *et al*., 2007), sporulation (Kimura *et al*., 2011), phage resistance (Nir-Paz *et al*., 2012), phage-induced and lysogenization (Kolot *et al*., 2008) and the cell cycle progression (Shapland *et al*., 2011).

In this study, we describe an unusual regulatory system where two interacting proteins with very different functions, the protein kinase PtkA and the transcription factor SalA, have arisen from the same ancestral domain (Walker motif ATPase). We report that the Mrp ATPase SalA is in fact a direct transcriptional regulator of *scoC* expression. It contains a hitherto unrecognized DNA-binding domain in its N-terminus, which allows it to bind upstream of the *scoC* gene. SalA DNA-binding is conditioned by the presence of ATP, and hence the SalA ATP-binding Walker motif and the DNA binding domain are functionally linked. Moreover, we demonstrate that the C-terminus of SalA engages in direct interaction with the BY-kinase PtkA. The consequence of this interaction is the phosphorylation of the residue tyrosine 327, situated in the SalA C-terminal domain. This phosphorylation activates SalA ATP binding and hydrolysis. This ultimately leads to more efficient binding of SalA to its target DNA, repression of *scoC* and overexpression of the exoprotease AprE.

Results and discussion

SalA is a DNA-binding protein that binds upstream of scoC

Bacillus subtilis SalA exhibits a modular architecture, commonly found in Mrp family ATPases (Hausmann *et al*., 2005). It possesses an ATP-binding Walker domain (Walker *et al*., 1982) situated between the residues 105–275 (Fig. 1A). Interestingly, the N-terminal region of SalA (residues 1–60) contains an unusually high proportion of lysines and arginines (12 out of 60 residues), indicating that it is likely to be positively charged. SalA has been shown to act as activator of *aprE* expression indirectly, via a negative effect on *scoC* (Ogura *et al*., 2004). Therefore, we asked whether the N-terminal region of SalA could exhibit DNA binding properties and bind upstream of *scoC* to repress it. In order to test this, we purified the SalA protein and prepared a 195 bp double-stranded DNA probe, containing the *scoC* promoter and 142 bp upstream. We performed an electrophoretic mobility-shift assay, attempting to detect SalA binding to this DNA fragment (Fig. 1B). The result was negative, with a very faint upward trend in the bands with increasing concentration of SalA, possibly indicating a very weak binding. Because the central region of SalA contains a putative ATP-binding domain, and most Walker motif-containing proteins are slow NTPases, we examined the ability of SalA to hydrolyze ATP. Purified SalA was indeed capable of slow ATP hydrolysis and exhibited a K_M value for ATP of 440 μM, and a k_{cat} of 0.3 s^{-1}. Next, we repeated the electrophoretic mobility-shift assay in the presence of 10 mM ATP. We chose this concentration as representative of high physiological ATP concentration in exponentially growing *B. subtilis*, based on several recent studies (Kleijn *et al*., 2010; Qi *et al*., 2014). In the presence of 10 mM ATP, SalA bound efficiently to the target DNA (Fig. 1B), suggesting that the presence of ATP is required for the interaction. In order to examine whether the 60 N-terminal residues of SalA indeed represent the DNA-binding domain, we constructed a mutant proteins with the 60 N-terminal amino acids deleted (SalA ΔNter) (Fig. 1A). SalA ΔNter could not bind the target DNA, even in the presence of 10 mM ATP (Fig. 1B). As the ATP binding/hydrolysis and the DNA binding functions are confined to distinct domains, it would seem plausible to presume that the ATP effect on DNA binding comes from a global conformational rearrangement. To assess this, we examined the SalA overall structural features by circular dichroism. The presence of 10 mM ATP induced a significant conformational change in SalA (Fig. 1C).

Next, we assessed the specificity of the SalA binding to the promoter region of *scoC*. We first asked whether SalA could bind the operator sequence of another *B. subtilis* transcription regulator, FatR (Gustaffson *et al*., 2001). The result was negative (Fig. S1). In a competition experiment with non-specific DNA, *E. coli* genomic DNA could not disrupt the binding of SalA to the labeled fragment containing the *socC* promoter (Fig. 2A), indicating that this interaction is indeed specific. The exact transcription start site of *scoC* was determined in the study by Abe *et al*. (2009), which also reported the binding site for the negative regulator TnrA, 144 bps upstream. In order to localize the SalA binding site, we decomposed our 195 bp frag-

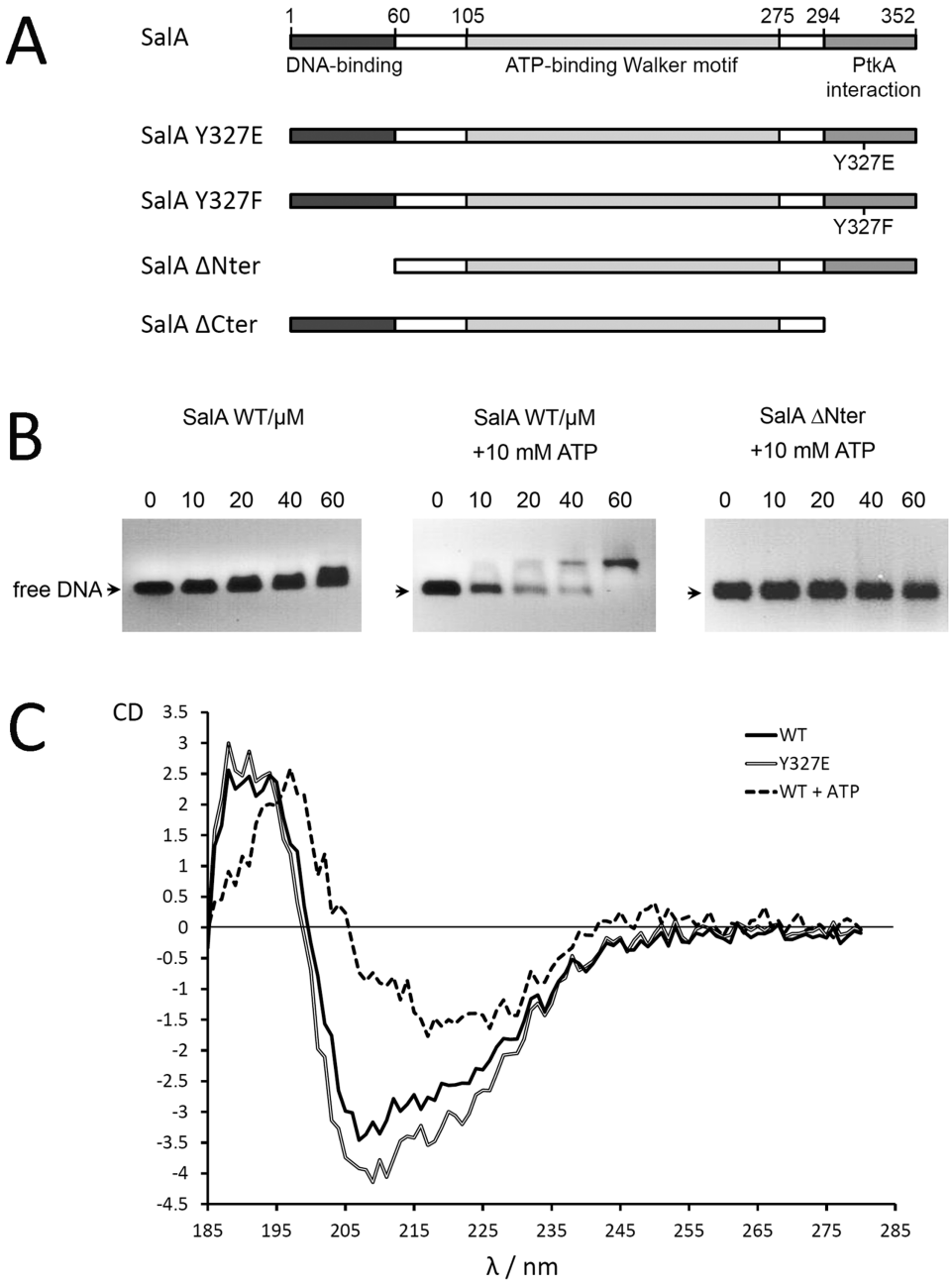

Fig. 1. SalA binds upstream of *scoC*, in the presence of ATP.
A. Schematic representation of the modular architecture of SalA, featuring the DNA-binding (residues 1–60), the ATP-binding (residues 105–275) and the PtkA-interaction (residues 294-35s) domain. Below the wild type SalA are different mutated versions used in this study.
B. *In vitro* gel-shift assays with SalA and SalA ΔNter (protein concentration in μM indicated above each lane). Prior to electrophoresis, proteins were incubated with fixed concentration (2 μM) of the 195 bp double stranded DNA fragment containing the operator sequence upstream of *scoC* (prepared by PCR, as described in *Experimental procedures*) and 10 mM ATP (when indicated). DNA was visualized with ethidium bromide staining.
C. Circular dichroism (CD) spectra of SalA (WT) alone, SalA in the presence of 10 mM ATP and SalA Y327E alone. The CD spectra shown for each protein correspond to the average of three continuous scans from 185 to 285 nm, collected at 20 nm/min (technical replicates).

ment into five regions of 39 bp each (Fig. 2B) and performed the electrophoretic mobility-shift assay with those. Only the two fragments closest to the 3′ end, containing the promoter region, were bound by SalA (Fig. 2B). We pursued the analysis with a series of progressively shorter DNA fragments (60, 40, 30 and 20 bps). SalA did not bind the 20 bp fragment, but it bound all other fragments. This suggested that the minimal binding site of SalA is situated

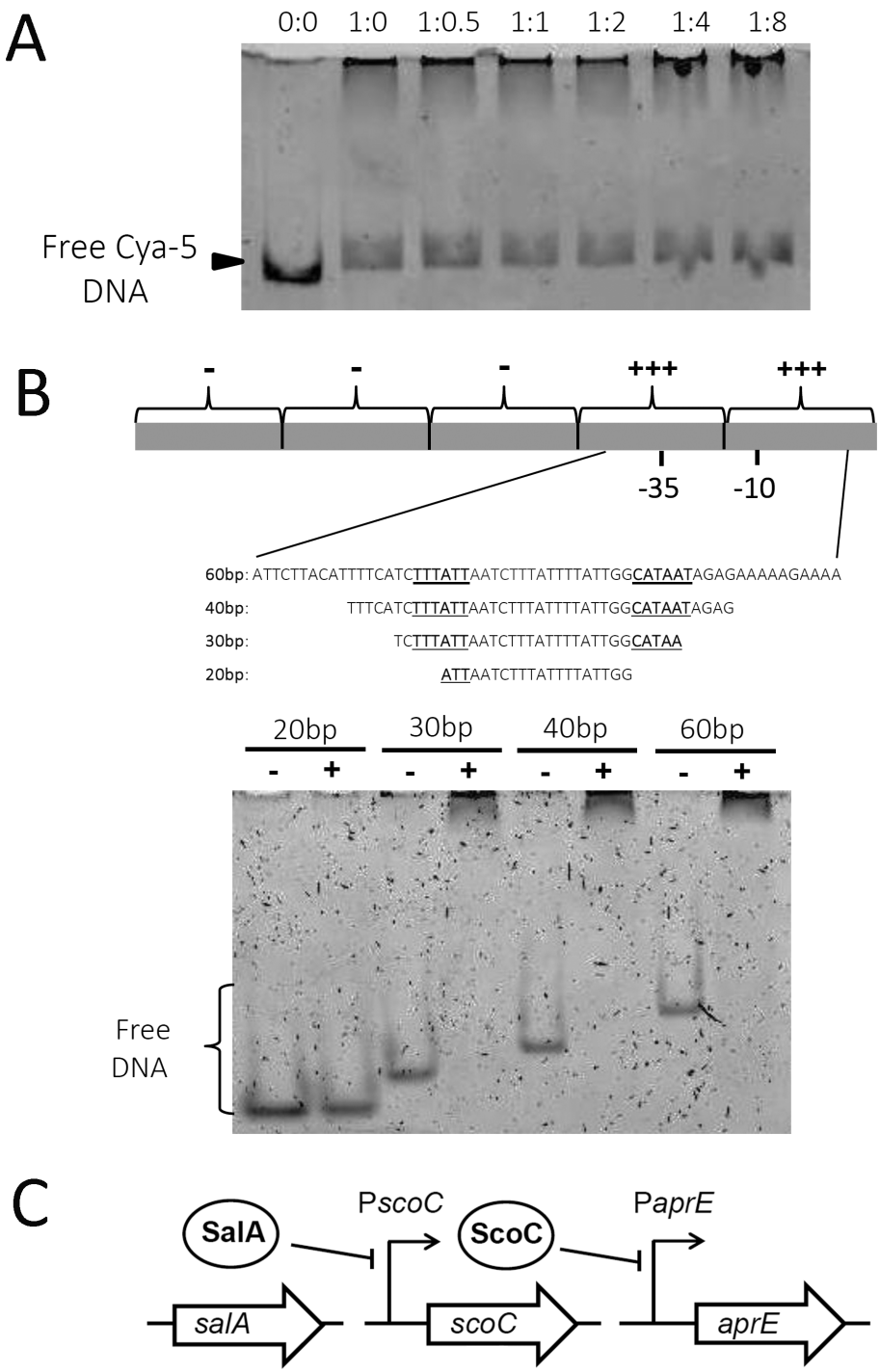

Fig. 2. SalA binds the *scoC* promoter specifically.
A. SalA electrophoretic mobility-shift assay with a 195 bp fluorescent double-stranded DNA probe labelled at 5′ with Cyanine 5, in competition with the genomic DNA purified from *E. coli* NM522. Above each lane, the ratio of the Cyanine 5 DNA probe (2 μM) and *E. coli* genomic DNA (ranging from 1 to 16 μM) is indicated.
B. Determination of the SalA binding site. The original 195 bp fragment (the gray bar) was divided into five 39 bp fragments, which were individually tested for electrophoretic mobility-shift assay in the presence of SalA. Above each fragment, the ability of SalA to bind it is indicated with +++/– signs. The 78 bp region bound by SalA was further shortened, to produce the 60, 40, 30 and 20 bp fragments, for which the sequence is shown. The –35 and –10 sites of the *scoC* promoter are highlighted in bold and underlined. The electrophoretic mobility-shift assay for these four fragments is shown, with the presence or absence of SalA indicated with + /– signs, respectively, above each lane.
C. Proposed clarification of the regulatory role of SalA as a repressor of *scoC*, which in turn represses the exoprotease gene *aprE* (Ogura *et al.*, 2004).

in the region -35 to -6, with respect to the *scoC* transcription start (the 30 bp fragment).

From these results, we concluded that the simplest explanation for the regulatory phenomenon observed by Ogura *et al*. (2004) is that SalA binds the *scoC* promoter to repress it and, in turn, alleviates the repression of ScoC on the exoprotease gene *aprE* (Fig. 2C). The role of AprE is the degradation of extracellular proteins, which allows *B. subtilis* to scavenge resources when nutrients become scarce. The regulation of *aprE* expression is complex; it involves other transcription factors besides ScoC (Ogura *et al*., 2003; 2004). ATP is clearly required to shift SalA into a distinct DNA-binding structural mode. However, the intracellular ATP concentration is unlikely to act as the physiological cue that controls the SalA repressor activity. AprE expression peaks in conditions when the cells are no longer growing exponentially (Nicolas *et al*., 2012), and the ATP levels are not at their peak value in those conditions.

The C-terminal domain of SalA (residues 294–352) interacts with the BY-kinase PtkA

In our recent interactomics study, SalA has been detected as an *in vivo* interactant of the *B. subtilis* BY-kinase PtkA (Shi *et al*., 2014b). In order to further characterize the SalA interaction with PtkA, we performed an additional two hybrid screen, which identified the 58 C-terminal residues of SalA (294–352) as the minimal interaction domain with PtkA (Fig. 3A). In this screen, the C-terminal domain of the PtkA activator TkmA, known to interact with the kinase (Mijakovic *et al*., 2003), was used as a positive control. As a negative control, we demonstrated that PtkA did not interact with its closest paralogue, the second *B. subtilis* BY-kinase, PtkB (EpsB) (Gerwig *et al*., 2014). The activation domain of the PtkA activator, TkmA, interacted with different versions of the kinase we tested (Fig. 3A), including the catalytically inactive PtkA K59M and PtkA D81A, the non-autophosphorylatable PtkA Y123F and phospho-mimetic PtkA Y123E (Mijakovic *et al*., 2003). By contrast, the SalA C-terminal domain was more selective (Fig 3A). Mutations of PtkA autophosphorylated tyrosines (Y123E and Y123F) did not affect the interaction with SalA, suggesting that the interaction does not depend on the phosphorylation state of the kinase. Conversely, mutations in the catalytic pocket of PtkA (D81A and K59M) abolished the interaction with SalA.

In order to confirm the two-hybrid findings using an independent approach, we performed a far-Western analysis. Purified proteins (indicated above each lane in Fig. 3B) were run on SDS-PAGE, blotted onto a membrane and incubated with Strep-tagged PtkA. PtkA interactants were revealed with a Strep-tactin HRP conjugate. TkmA–PtkA interaction is shown as a positive control, and BSA as a negative control. Wild-type SalA interacted with

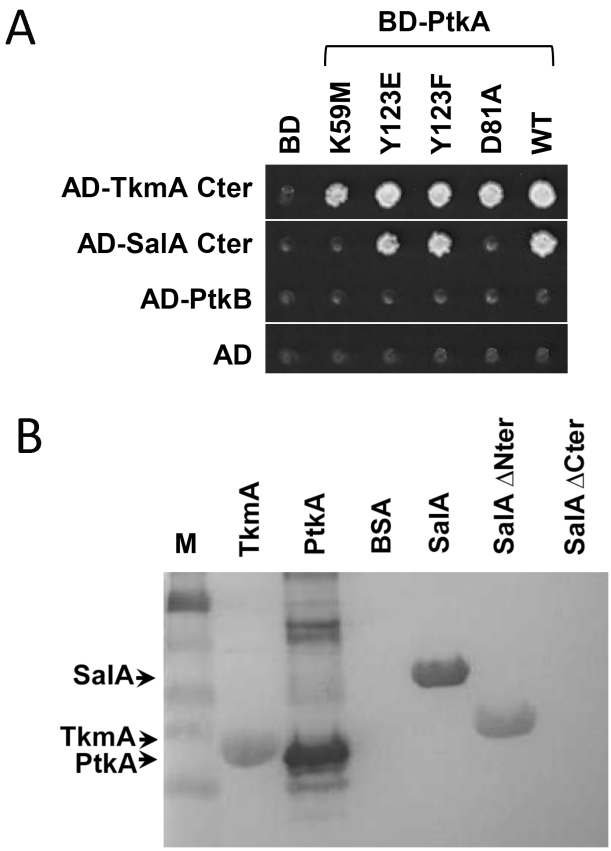

Fig. 3. C-terminus of SalA interacts with PtkA.
A. Interaction between PtkA and the C-terminal domain of SalA in yeast two-hybrid. A and α haploid strains expressing the BD- (left) and AD- (top) protein fusions as indicated were mixed to form diploids. The interaction phenotypes upon coexpression of two protein fusions were assayed by the ability of the diploids cells to grow on -LUH selective media. Negative controls include the absence of interaction phenotype between PtkA and PtkB as well as the absence of auto-activating phenotypes when PtkA is coexpressed with the Gal4-AD domain alone (AD). TmkA C terminal domain was used as a positive control.
B. Far-Western analysis detection of PtkA interactants. Individual proteins (indicated above each lane, 'M' stands for size marker) were separated by SDS-PAGE, blotted onto a PVDF membrane and incubated with Strep-tagged PtkA. Proteins interacting with PtkA were detected using the Strep-tactin HRP conjugate. BSA was used as a negative control.

PtkA, and the loss of its N-terminal DNA-binding domain (residues 1–60) (SalA ΔNter) had no bearing on the interaction. By contrast, the loss of the C-terminal extension (residues 294–352) (SalA ΔCter), abolished the interaction completely (Fig. 3B). This was in agreement with the two-hybrid result, where this region was identified as the minimal interaction domain.

SalA is phosphorylated at the residue Y327 by the BY-kinase PtkA

The specific interaction between PtkA and SalA, and the similarity of their ATP-binding domains (Mijakovic *et al*.,

Fig. 4. SalA is phosphorylated by PtkA.
A. *In vitro* phosphorylation assay with purified SalA, PtkA and TkmA. The presence of 1 μM proteins (PtkA, TkmA and SalA) is indicated above each lane. Reactions were incubated for 30 min in the presence of ^{32}P-γ-ATP, run on SDS-PAGE, and signals were revealed by autoradiography.
B. *In vitro* phosphorylation assay with *B. subtilis* SalA and PtkA homologues (BY-kinases) from other bacteria. Presence of purified proteins in each lane, 1 μM *B. subtilis* SalA and BY-kinases from different bacteria, is marked with '+'. Lanes labelled '*K. pneumo*' contain 1 μM BY-kinase from *K. pneumoniae*, lanes labeled '*S. aureus*' contain 1 μM BY-kinase from *S. aureus* (CapAB), and lanes labeled '*S. pneumo*' contain 1 μM BY-kinase from *S. pneumoniae* (CpsCD). Reactions were incubated for 30 min in the presence of ^{32}P-γ-ATP, run on SDS-PAGE, and signals were revealed by autoradiography.
C and D. Mass spectrometry analysis of phosphorylated SalA. After *in vitro* phosphorylation by PtkA, in the presence of non-radioactive ATP, the sample was digested in solution with trypsine. Phosphopeptides were enriched by TiO_2 chromatography and analyzed by mass spectrometry. The spectra show the fragmentation pattern of the SalA peptides phosphorylated at Y278 (C) and Y327 (D).
E. *In vitro* phosphorylation assay with mutated versions of SalA. Each lane contains 1 μM PtkA, except lane 8, which contains One micromolar of catalytically inactive PtkA K95M. One micromolar of TkmA is present only in lane 1. One micromolar versions of SalA are present as follows: wild type SalA in lanes 1, 2 and 8, SalA Y327 F in lane 3, SalA Y327E in lane 4, SalA Y278F in lane 5, SalA ΔNter in lane 6 and SalA ΔCter in lane 7. Reactions were incubated for 30 min in the presence of ^{32}P-γ-ATP, run on SDS-PAGE, and signals were revealed by autoradiography. (F) *In vitro* dephosphorylation assay with PtpZ. SalA was phosphorylated for 30 min in the presence of with ^{32}P-γ-ATP as described above. All lanes contain 1 μM PtkA and 3.5 μM SalA. Five micromolar of PtpZ was added at time zero, and the reactions were stopped by adding the SDS-PAGE loading buffer, at time points indicated above each lane. Radioactive signals of phosphorylated proteins were revealed by autoradiography.

2005) opened up two questions: can SalA be a substrate of PtkA, and can SalA itself act as a kinase? To investigate this, *in vitro* phosphorylation assays were performed with purified proteins. SalA alone could not autophosphorylate (Fig. 4A, lane 3), nor could it phosphorylate the catalytically inactive form of PtkA (Fig. 4E, lane 8). We therefore concluded that it is not a *bona fide* BY-kinase. However, in the presence of PtkA, SalA was phosphorylated, prompting us to conclude that SalA is a substrate of PtkA (Fig. 4A). Interestingly, SalA could be phosphorylated by PtkA also in the absence of TkmA (Fig. 4A). This finding is somewhat unusual, as PtkA requires the presence of TkmA to phosphorylate other known substrates (Mijakovic *et al*., 2003; 2006; Jers *et al*., 2010; Derouiche *et al*., 2013). In order to evaluate whether SalA phosphorylation by PtkA is confined only to *B. subtilis*, we purified previously characterized PtkA homologues from *Streptococcus pneumoniae* (Henriques *et al*., 2011), *Staphylococcus aureus* (Soulat *et al*., 2006) and *Klebsiella pneumoniae* (Preneta *et al*., 2002) and tested their ability to phosphorylate *B. subtilis* SalA *in vitro*. All tested BY-kinases phosphorylated SalA, with a varying degree of efficiency (Fig. 4B), indicating that this kinase–substrate relationship is conserved across species boundaries. The next step was to identify the phosphorylation site(s) on SalA. SalA phosphorylated *in vitro* by PtkA was submitted to mass spectrometry analysis. Phosphorylation was unambiguously detected on residues Y278 and Y327 (Fig. 3C and D). Because mass spectrometry is a very sensitive method and picks up low occupancy sites, we individually point-mutated these two residues to non-phosphorylatable phenylalanine, to assess the extent of their phosphorylation. The non-phosphorylatable mutant Y278F retained wild-type level of *in vitro* phosphorylation (Fig. 4E, lane 5), indicating that this site, situated in a poorly conserved region downstream of the ATP-binding domain, is of very low occupancy. By contrast, SalA Y327F lost over 95% of the phosphorylation signal (Fig. 4E, lane 3), suggesting that this site, situated in the C-terminal extension downstream of the ATP-binding domain, is of major importance. Y327 is in the middle of the SalA C-terminal region (residues 294–352) that interacts with PtkA (Fig. 3), so the finding that it is the major phosphorylated residue is in accordance with its location. The deletion of the DNA-binding N-terminal domain of SalA (SalA ΔNter) had no impact on phosphorylation by PtkA (Fig 4E, lane 6). As expected, the deletion of residues 294–352 in the SalA ΔCter led to a complete loss of phosphorylation (Fig 4E, lane 7). We concluded that the interaction between PtkA and the C-terminal domain of SalA leads to phosphorylation of the SalA residue Y327 by the kinase. Substrates of PtkA are typically dephosphorylated by the cognate phosphotyrosine-protein phosphatase PtpZ (Mijakovic *et al*., 2005). Phosphorylated SalA was also efficiently dephosphorylated by PtpZ *in vitro* (Fig. 4F).

Next, we used the octameric structure of the BY-kinase CapAB (PDB ID 2VED) (Olivares-Illana *et al*., 2008) as a framework to propose the mode of interaction between SalA and PtkA (Fig. 5A). In the model of the SalA-PtkA hetero-dimer, the phosphorylatable SalA residue Y327 is facing directly toward the active site of PtkA. This model supports the notion that the C-terminus of SalA interacts with the active site of PtkA and that the major phosphorylation residue Y327 is on the interaction surface and accessible to the kinase. Y327 is also very near the ATP binding site of SalA, and a conformational change triggered by its phosphorylation could easily extend via the short helix (Fig. 5A, orange helix in the SalA structure) to the ATP binding site. Interestingly, the residue Y327 is conserved in all SalA-like proteins in *Bacilli*, and in the SalA homologue from *S. aureus* (Fig. 5B). However, there are no direct SalA homologues in *S. pneumoniae* and

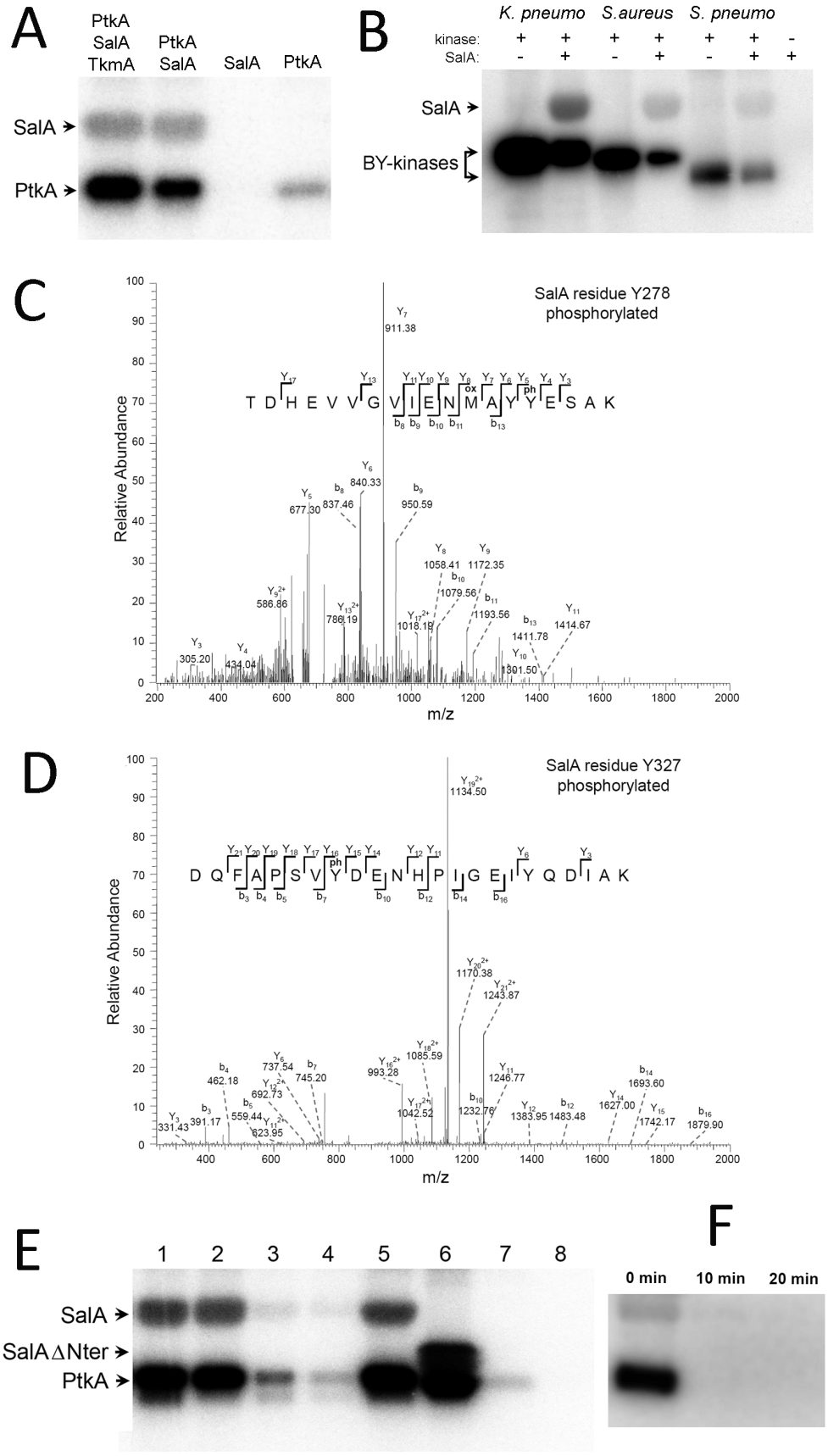
A
PtkA
SalA
TkmA
PtkA
SalA
SalA
PtkA
SalA
PtkA
B
K. pneumo
S.aureus
S. pneumo
kinase:
SalA:
SalA
BY-kinases
C
SalA residue Y278 phosphorylated
Relative Abundance
m/z
T D H E V V G V I E N M A Y Y E S A K
ox
ph
911.38
840.33
677.30
837.46
950.59
1058.41
1172.35
1079.56
1193.56
1414.67
1411.78
1391.50
1018.18
786.19
586.86
305.20
434.04
D
SalA residue Y327 phosphorylated
Relative Abundance
m/z
D Q F A P S V Y D E N H P I G E I Y Q D I A K
ph
1134.50
1170.38
1243.87
1085.59
737.54
745.20
462.18
692.73
993.28
1246.77
1693.60
1627.00
1742.17
1879.90
1232.76
1383.95
1483.48
1042.52
559.44
623.95
391.17
331.43
E
1 2 3 4 5 6 7 8
SalA
SalAΔNter
PtkA
F
0 min
10 min
20 min

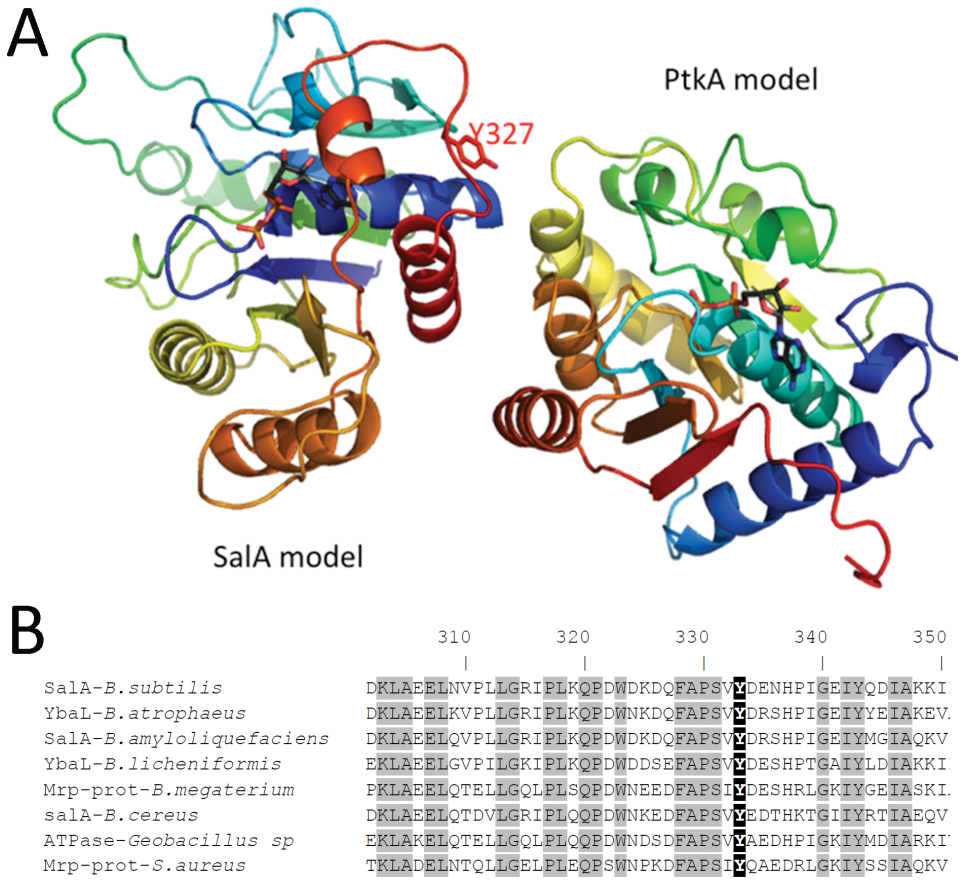

Fig. 5. The phosphorylated residue Y327.
A. Model of the PtkA-SalA interaction. The model of SalA obtained using MinD as template has been superimposed on the CapAB subunit 1 and the model of PtkA obtained using CapB as model has been superimposed on subunit 2. The phosphorylatable residue of SalA Y327 is highlighted in sticks and labeled. The figure has been prepared using PyMol (Seeliger and de Groot, 2010).
B. Protein sequence alignment of the C-termini of SalA protein orthologues (Mrp family regulators) from *Bacillus subtilis*, *Bacillus atrophaeus*, *Bacillus amyloliquefaciens* DSM7, *Bacillus licheniformis* DSM13, *Bacillus megaterium* DSM319, *Bacillus cereus*, *Geobacillus sp* and *Staphylococcus aureus*. The tyrosine corresponding to the residue 327 in the *B. subtilis* SalA is highlighted by the black box.

K. pneumoniae. The Mrp proteins from these bacteria are too distant to support a full-length sequence alignment, and there is no evident equivalent of the residue Y327.

SalA phosphorylation at the residue Y327 leads to more efficient binding to the target DNA and overproduction of the exoprotease AprE

The next question we addressed was the functional consequence of SalA phosphorylation at the residue Y327. As we have established that SalA is a DNA-binding protein, we examined the influence of SalA phosphorylation on binding its target DNA (Fig. 6A). In this assay we lowered the SalA concentration 10-fold compared with Fig 1B, so that even in the presence of 10 mM ATP, 6 μM non-phosphorylated SalA did not shift the DNA (Fig. 6A). However, 6 μM SalA pre-phosphorylated by PtkA shifted the DNA entirely (Fig. 6A), in the presence of 10 mM ATP. This suggested that phosphorylation of SalA stimulates its DNA binding activity. As the phosphorylation site (Y327) and the DNA binding domain (residues 1–60) are on the opposite ends of the protein, we speculated that the effect of phosphorylation on DNA binding might involve the ATP-binding domain which is in between. We have already established that SalA DNA-binding depends on the presence of ATP (Fig. 1B). Therefore, we asked whether phosphorylation of SalA Y327 could influence ATP binding or hydrolysis. As it is not possible to reach 100% phosphorylation of SalA *in vitro*, or control the phosphorylation level precisely, we opted to use the phospho-mimetic mutant SalA Y327E to obtain reproducible kinetics data. We first verified by circular dichroism that the Y327E mutation did not cause any structural perturbations and were satisfied that the CD spectra of WT and Y327E SalA were almost identical (Fig. 1C). The phospho-mimetic SalA Y327E exhibited higher affinity for ATP (K_M = 69 μM)

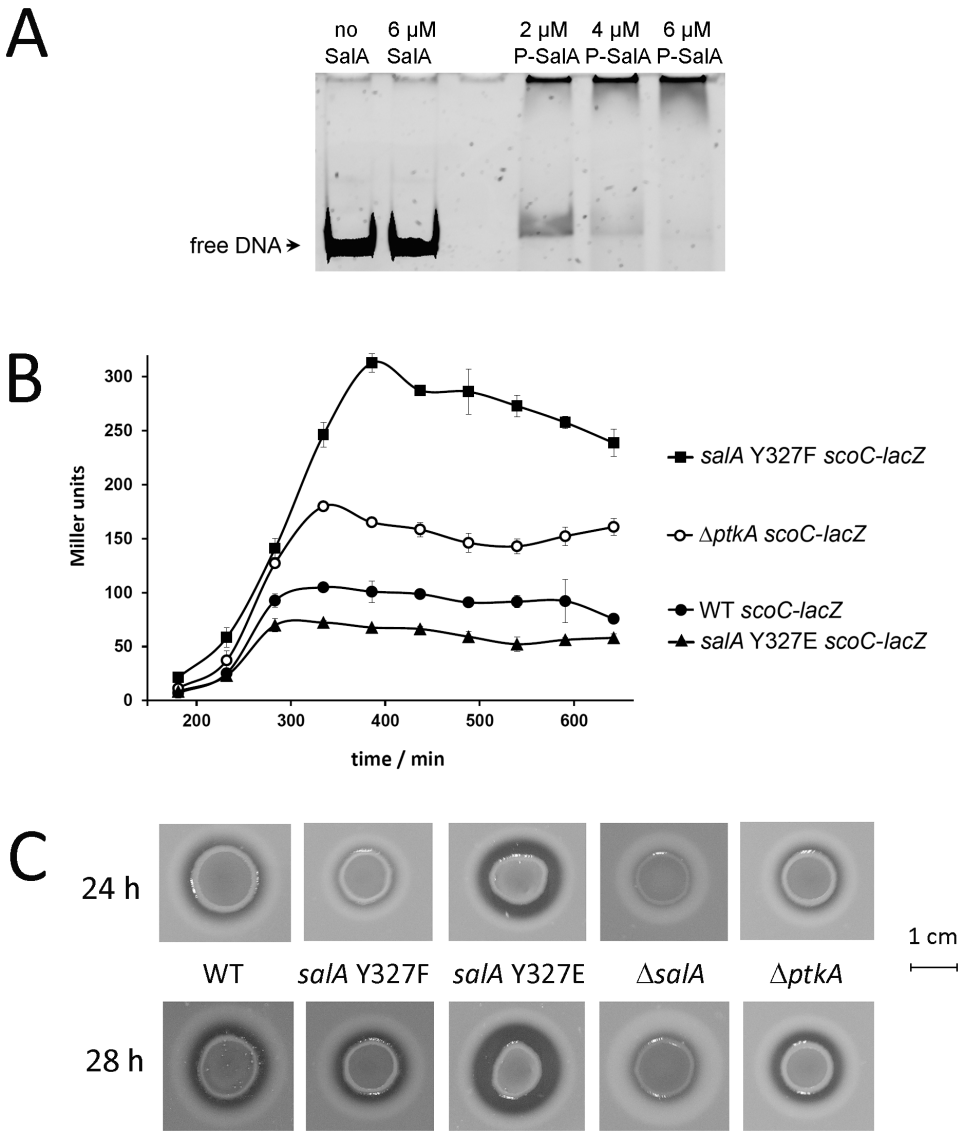

Fig. 6. Phosphorylation of SalA increases its binding to target DNA, represses *scoC* and induces *aprE* expression.
A. *In vitro* gel-shift assay with SalA and pre-phosphorylated SalA. SalA was pre-incubated for 45 min at 37°C with 10 mM ATP in either the presence or absence of 1 µM PtkA (to pre-phosphorylate SalA). Ten micromolar ATP was kept in all reactions to ensure the same reference point. Samples shown in all lanes were subsequently incubated for 15 min with 2 µM of the 195 bp double stranded DNA fragment containing the operator sequence upstream of the *scoC* (prepared by PCR, as described in *Experimental procedures*) and 10 mM ATP. Presence and concentration of SalA is indicated above each lane, 'P-SalA' stands for pre-phosphorylated SalA. The samples were separated by electrophoresis, and DNA was visualized with ethidium bromide staining.
B. Beta-galactosidase assays performed with *scoC*::*lacZ* in four different backgrounds: wild type (filled circles), Δ*ptkA* (open circles), *salA* Y327F (filled squares) and *salA* Y327E (filled triangles). The result shown here is one representative experiment with three technical replicates.
C. Exoprotease production of strains WT, *salA* Y327F, *salA* Y327E, Δ*salA* and Δ*ptkA*, on the DS medium with 1.5% skimmed milk. The extracellular protease production was measured by the diameter of the hydrolytic halo around the colony (hours after inoculation are indicated to the left). The results shown are representative samples from three biological replicates.

and hydrolyzed ATP faster (k_{cat} = 2.6 s^{-1}) (compared to WT SalA, KM = 440 µM, kcat = 0.3 s^{-1}). This suggested that phosphorylation-based activation of SalA DNA binding is indeed related to stimulation of its ATP binding and/or hydrolysis. Next, we examined the effect of the SalA Y327E mutation *in vivo*. We probed the expression from the *scoC* promoter, using the *lacZ* reporter gene (Fig. 6B). As expected, the replacement of the *salA* allele with *salA* Y327E led to a tighter repression of *scoC*. Conversely, inactivation of *ptkA* or introduction of a non-phosphorylatable mutation *salA* Y327F led to higher expression of *scoC*. Tight repression of *scoC* in *salA*

Y327E should be expected to lead to induction of *aprE*. This is exactly what was observed in the exoprotease assay (Fig. 6C). The strain harboring *salA* Y327E produced a significantly larger halo of hydrolyzed milk compared with the WT, whereas the negative controls Δ*salA*, *salA* Y327F and Δ*ptkA* exhibited the opposite effect (in decreasing order of intensity). Although *aprE* overexpression was the most apparent consequence of SalA phosphorylation, it might not be the only one. To assess other possible phenotypes related to SalA phosphorylation, we examined the localization of C-terminal GFP fusions of SalA, SalA Y327E and SalA Y327F (Fig. S2). They all exhibited a diffuse cytosolic localization. However, in 19% of the examined WT cells, a single bright SalA-GFP focus could be observed. The occurrence frequency of these foci was reduced to 10% of the examined cells in the strain bearing SalA Y327F and increased to 26% of the examined cells for SalA Y327E (Fig. S2). The physiological significance of these foci remains to be elucidated.

Concluding remarks

Domain duplication, driven by stochastic recombination events (Vogel *et al.*, 2005; Vogel and Morea, 2006), is one of the widely acknowledged evolutionary mechanisms for increasing protein complexity (Rydén and Hunt, 1993). The typical consequence of duplication is convergent evolution, in which duplicated domains evolve separately to accomplish new physiological roles in the cell (Van Damme *et al.*, 2007). One recognized constraint for evolving new proteins via domain duplication is the preservation of the interfaces for protein–protein interactions (Heringa and Taylor, 1997). Our results point to the ATP-binding domain duplication in *B. subtilis*, which has led to emergence of a transcription factor SalA and a protein kinase PtkA. Divergent evolution involved the addition of functional domains (DNA-binding domain for SalA, BY-kinase autophosphorylation domain for PtkA) that resulted in two proteins that accomplish very different cellular roles. Despite different architectures and present day functions, SalA and PtkA have obviously retained the interaction interface, leading to PtkA-dependent regulatory phosphorylation of SalA. The transcription levels of *ptkA* and *salA* correlate in about 35% of the growth conditions examined by Nicolas *et al.* (2012), supporting a functional correlation. In this study, we have focused on the expression of *aprE* as the functional consequence of SalA binding to the promoter of *scoC*. However, *scoC* is known to control other transition phase functions, such as the synthesis of bacilysin, encoded by the operon *bacA-F* (Inaoka *et al.*, 2009). Phosphorylation of SalA is likely to affect other targets of ScoC, and this should be explored in further studies. We have ascertained that other types of BY-kinases from *S. pneumoniae*, *S. aureus* and *K. pneumoniae* can phosphorylate SalA, indicating that this regulatory interaction could be maintained in other bacteria, and therefore be of general significance.

Experimental procedures

Bacterial strains and growth conditions

Escherichia coli NM522 was used for gene cloning. The chaperone overproducing strain *E. coli* M15 carrying pREP4-*groESL* (20) was used for overproduction of proteins. *B. subtilis* BS514 (*B. subtilis* 168 *trp* + Pr::*neoR*) was used for *in vivo* mutant construction, and its derivatives used in this study are listed in Table S1. *E. coli* and *B. subtilis* strains were grown in Luria–Bertani (LB) medium with shaking, at 37°C. When relevant ampicillin (100 μg ml^{-1}) and kanamycin (25 μg ml^{-1}) for *E. coli* and erythromycin (1 μg ml^{-1}), neomycin (5 μg ml^{-1}), phleomycin (2 μg ml^{-1}), chloramphenicol (5 μg ml^{-1}) and spectinomycin (100 μg ml^{-1}) for *B. subtilis* were added to the medium.

DNA manipulation and strain construction

All PCR primers with restriction enzymes are listed in Table S2. Gene *salA* was PCR-amplified from *B. subtilis* 168 genomic DNA and inserted between the BamHI and HinDIII sites of the vector pQE-30 (Qiagen). Gene *salA* was inserted into the vector pSG1729 (21) between KpnI and XhoI sites, resulting in a replacement of the *gfp* gene downstream the Pxyl by *Strep-salA*. The point-mutations *salA* Y278F, *salA* Y327F and *salA* Y327E were obtained using two partially overlapping mutagenic primers. Truncated version of *salA*: *salA* ΔNter (deletion of residues 1–60) and *salA* ΔCter (deletion of residues 294–352) were obtained using complementary primers inside the gene sequence. Construction of the non-phosphorylatable *salA* Y327F and the phospho-mimetic *salA* Y327E mutants at natural *salA* locus was performed using the modified mutation delivery method of Fabret *et al.* (2002) (22). Briefly, the DNA fragments were amplified from the *B. subtilis* 168 chromosome using the pairs of primers *salA*fwd/*salA*327F-R and *salA*327F-F/*salA*rev for the Y327F mutation and *salA*fwd/*salA*327E-R and *salA*327E-F/*salA*rev for the Y327E mutation. Using primers *salA*fwd and *salA*rev, these fragments were PCR-joined to the insertion cassette containing the phage lambda *cI* repressor gene and the phleomycin resistance marker. The resulting PCR products were used to transform the competent BS514 cells expressing neomycin resistance gene from lambda promoter, negatively controlled by the *cI* repressor. The transformants were selected for the phleomycin resistance and neomycin sensitivity. Finally, the counter-selection for neomycin resistance and phleomycin sensitivity was applied to select clones which had lost the insertion cassette from the chromosome via recombination between the flanking direct repeats. The deletion of *salA* gene was performed similarly using the pairs of primers *salA*fwd/*salA*rev (Table S2). The partially complementary primers Δ*salA* fwd/Δ*salA* rev were designed to introduce an in-frame deletion between codons 10 and 343. The C-terminal fusions of different forms of SalA with fluorescent GFP were constructed using oligonucleotides *SalA*int1164 and *SalA*end1164 and the chromosomes of the following

B. subtilis strains: WT 168, *salA* Y327E, and *salA* Y327F as templates for PCR. The amplified DNA fragments were cloned between the ApaI and SalI sites of the pSG1164 vector and the resulting plasmids were used to transform the respective *B. subtilis* strains. Transformants were selected for chloramphenicol resistance. For *lacZ* fusion with *scoC*, a 0.5 kb fragment corresponding to the central region of *scoC* was PCR-amplified from genomic DNA and inserted between the EcoRI and BamHI sites of pMUTIN2. *B. subtilis* wild type, Δ*ptkA* (15), *salA* Y327F and *salA* Y327E were transformed with this pMUTIN2 construct and selected for erythromycin resistance. All constructs were verified by sequencing.

Yeast two hybrid

Coding sequences *ptkA* and *tkmA* were PCR-amplified from the *B. subtilis* 168 genomic DNA and cloned in fusion with the DNA-binding domain (BD) and activation domain (AD) of Gal4 in the bait and prey vectors pGBDU-C1 and PGAD-C1 respectively (23). Constructions were carried out in *E. coli* and sequenced prior to the introduction in PJ69-4a (for pGBDU derivatives) or pJ69-4a (for PGAD derivatives) yeast haploid strains. Yeast two-hybrid assays were performed as follows. First, the BD-PtkA fusion was used to screen the *B. subtilis* yeast two-hybrid library as described previously (24). Positive clones were identified by PCR amplification and sequencing of the AD-fused prey DNA. The prey candidates were then re-introduced into the pGAD vector by gap repair, after co-transformation of the PCR-amplified inserts with the linearized pGAD vector into the PJ169-4a haploid strain. Then, The PJ169-4a and pJ169-4a strains carrying different bait and prey constructs were mated in a 2×2 matrix. Diploids were selected on selective media (-LU), and the interaction phenotypes were assayed by their ability to grow on -LUH and -LUA selective media, as described by James *et al*. (1996) (23). Interactions were considered as specific when reproduced twice independently and not associated with auto-activation of the phenotypes or the stickiness properties of the prey proteins.

Synthesis and purification of tagged proteins

All SalA mutant proteins were synthesized as 6xHis N-terminal fusions in *E. coli* M15 harboring pREP4-*groESL*, except for 6xHis-SalA wild type which was overproduced directly in *E. coli* NM522. Cultures were grown with shaking at 37°C to OD_{600} of 0.5, expression was induced with 1 mM IPTG and cells were grown for an additional 3 h. 6xHis-tagged proteins were purified on Ni-NTA columns (Qiagen) as described previously (11). Strep-tagged proteins were purified by Strep Tactin affinity chromatography (Novagen) as described previously (25). Protein aliquots were stored at −80°C in a buffer containing 50 mM Tris-Cl pH 7.5, 100 mM NaCl and 10% glycerol.

In vitro *phosphorylation and dephosphorylation assays*

Phosphorylation assays were performed essentially as described previously for substrates of *B. subtilis* PtkA and TkmA (11). A typical 40 µl reaction contained 1 µM PtkA, 1 µM TkmA-NCter (optional, indicated in the figure legends), 5 µM SalA or mutated versions thereof, 50 µM [γ-^{32}P] ATP (20 µCi mmol^{-1}), 1 mM $MgCl_2$ and 100 mM Tris-HCl pH 7.5. The same reaction was repeated by replacing PtkA from *B. subtilis* by BY-kinases from *K. pneumoniae*, *S. aureus* and *S. pneumoniae*. When the reaction composition varied with respect to this protocol, the composition is indicated in the figure legends. Reactions were incubated at 37°C for 30 min and stopped by adding SDS-PAGE loading buffer and heating at 100°C for 5 min. Proteins were separated by electrophoresis on SDS-PAGE (12% polyacrylamide), then washed by boiling in 0.5 M HCl for 10 min to reduce the background and dried. Autoradiography signals were visualized with a PhosphoImager (FUJI). All experiment was repeated three times with proteins purified independently, and the results were identical. In each case one representative experiment is shown. For the dephosphorylation assay with PtpZ, SalA was first phosphorylated as described above, and then incubated with 5 µM PtpZ. The samples were treated as described above, and the radioactive signals of phosphorylated proteins were revealed by autoradiography.

Mass spectrometry analysis of phosphorylation sites

One hundred micrograms of 6xHis-SalA wild type protein were phosphorylated *in vitro* using the protocol described above (with non-radioactive ATP). Purified SalA was digested in solution with trypsin as described by Borchert *et al*. (2010) (26). Ten percent of the peptide mixture was desalted using C18 StageTips (27) and analyzed directly by LC-MS/MS. The remaining 90% of the peptide mix was subjected to phosphopeptide enrichment by TiO_2 chromatography as described previously (28), with minor modifications (13). Analysis of peptides and phosphopeptides was done on a Proxeon Easy-LC system (Proxeon Biosystems, Denmark) coupled to a LTQ-Orbitrap-XL (Thermo Fisher Scientific, Germany) equipped with a nanoelectrospray ion source (Proxeon Biosystems, Denmark) as described by Koch *et al*. (2011) (29). The five most intense precursor ions were fragmented by activation of neutral loss ions at –98, –49 and –32.6 relative to the precursor ion (multistage activation). Mass spectra were analyzed using the software suite MaxQuant, version 1.0.14.3 (30). The data were searched against a target-decoy *E. coli* database including the 6xHis-FatR sequence and 262 common contaminants. Phosphorylation of serine, threonine and tyrosine were set as variable modifications, besides N-terminal acetylation and oxidation of methionine. Carbamidomethylation of cysteine was set as fixed modification. Initial precursor mass tolerance was set to 7 ppm at the precursor ion and 0.5 Da at the fragment ion level. Phosphorylation events with a localization probability of at least 0.75 were considered to be assigned to a specific residue.

DNA-binding assay

Initial SalA electrophoretic mobility-shift assays were performed with a 195 bp double-stranded DNA probe, which was PCR-amplified from the *B. subtilis* genomic using the primers salA-shi-fw and salA-shi-rev (Table S2), and the probe contains the *scoC* promoter and 142 bps upstream. Different ratios (indicated in the figure legend) of the DNA probe (all reactions contained 2 µM DNA) and SalA (or SalA ΔNter) were mixed with 25 mM Tris-HCl pH 7.5, 50 mM NaCl, 5% glycerol and 10 mM $MgCl_2$. Ten micromolar ATP was optional

(indicated in the figure legends). Reactions were incubated for 30 min at 37°C and loaded on a 1.5% agarose gel with 0.5 μg ml^{-1} of ethidium bromide. Migration was performed for 2 h at 2 V cm^{-1} in 0.5× Tris-acetate-EDTA. The electrophoretic mobility-shift assays with shorter DNA fragments were performed in the identical setup. All experiments were repeated three times with proteins purified independently, and the results were identical. One representative experiment is shown. For the competition assays, the labeled version of the same 195 bp DNA probe was prepared by PCR, using the primers salA shi cya5-fw and salA-shi-rev. The probe was mixed with SalA and the *E. coli* genomic DNA in the buffer containing 25 mM Tris-HCl pH 7.5, 50 mM NaCl, 5% glycerol, 10 mM MgCl2 and 10 mM ATP. Reactions were incubated for 30 min at 37°C and loaded on a native 8% polyacrylamide gel (without SDS). For the competition assay, the labeled DNA probe was visualized by incubating the gel for 20 min with shaking in 30 ml of the Tris-glycine buffer (2.5 mM Tris, 192 mM glycine) with 15 μl of the gel green nucleic acid stain (Biotium). In all other assays (agarose or polyacrylamide gels), the DNA fragment was visualized with ethidium bromide staining.

β-galactosidase assay

One hundred milliliters of LB were inoculated with overnight *B. subtilis* culture to a final OD_{600} of 0.025 and grown with shaking at 37°C. At time points indicated in the figure, 2 ml samples were taken, spun down (2 min at 10 000 *g*) and cell pellets were stored at –20°C. Pellets was resuspended in 0.5 ml Z-buffer (60 mM Na_2HPO_4·7H20, 40 mM NaH_2PO_4·H_20, 10 mM KCl, 1 mM $MgSO_4$ and 50 mM β-mercaptoethanol, pH 7.0). The 0.5 ml of cell suspension were treated with 30 μg ml^{-1} lysozyme and 3 μg ml^{-1} DNase for 15 min at 37°C. Reaction was started by addition of 0.2 ml of 4 mg ml^{-1} ortho-nitrophenyl-β-galactoside and stopped with 0.5 ml of 1 M Na_2CO_3. Three biological replicates were performed, yielding similar results. One representative biological replicate is shown, with standard deviations from three technical replicates.

Protease assay

Cells were grown overnight at 37°C on the DS medium (8 g nutrient broth, 0.25 g $MgSO_4$·7H2O, 1 g KCl, 1 ml $Ca(NO_3)_2$ (1 mM), 1 ml $MnCl_2$ (10 mM), 1 ml $FeSO_4$ (1 mM) dissolved in 1 liter final volume). Cells were then inoculated in preheated DS medium at OD_{600} of 0.02 and grown to mid-late exponential phase. Two microliters of culture were spotted onto DS agar plates [with 1.5% (w/v) skimmed milk and 1.5% (w/v) agar]. The plates were incubated at 37°C. The diameter of the hydrolytic halo surrounding the colony indicates extracellular protease productivity (31). Three biological replicate of the experiments were performed, with identical results. One representative result is shown.

Circular dichroism measurements

All circular dichroism experiments were performed on a Chirascan CD Spectrometer at 20°C in a 0.2 mm path length cuvette (106-QS, Hellma Analytics). SalA and SalA Y327E were dialyzed against 50 mM ammonium bicarbonate and lyophilized. The lyophilized samples were resuspended in 25 mM HEPES, pH 7.5, to a final concentration of 1.5 mg ml^{-1}. Two hundred fifty nanomolar solution of each protein was used for the measurements. The CD spectra shown for each protein correspond to the average of three continuous scans from 185 to 285 nm, collected at 20 nm min^{-1}. Background spectra with or without ATP were recorded and subtracted accordingly. The data were processed using Global 3™ Analysis Software from Chirascan.

ATPase assay

ATPase activity assays were performed using an assay coupled to NADH oxidation. The reaction mixture contained: 2.5 nM SalA or SalA Y327E, 2 mM phosphoenolpyruvate (Sigma), 0.16 mM NADH, 5U of pyruvate kinase and 8U of lactate dehydrogenase (Sigma), 50 mM potassium-HEPES pH 7.5, 150 mM potassium acetate, 8 mM magnesium acetate, 5 mM β-mercaptoethanol and 250 μg ml^{-1} bovine serum albumin. Reactions were incubated for 5 min at 37°C, and varying concentrations of ATP (Sigma) were added to initiate the reaction. Oxidation of NADH was followed at 340 nm. Hanes-Woolf linearization of the kinetics data was used to calculate the K_M and k_{cat} values from three technical replicates.

Far-Western blot

Proteins to be tested for interaction with PtkA were separated on 12% SDS-PAGE gel. Proteins were blotted to a PVDF membrane with Trans-blot cell (Bio-Rad) in a buffer containing 25 mM Tris, 125 mM glycine pH 8.3 and 10% ethanol. The membrane was blocked with 5% bovine serum albumin in TBS-T buffer (25 mM Tris pH 8, 125 mM NaCl, 1% Tween 20) for 1 h at room temperature, and then incubated with 10 nM Strep-tagged PtkA. To reveal the interactants, membrane was incubated with 1:1000 of Strep-tactin HRP conjugate (IBA BioTagnology) for 1 h in TBS-T buffer containing 1% BSA. Signals were detected using an enhanced chemiluminescence AEC Chromagen kit (SIGMA). The experiment was repeated three times with proteins purified independently, and the results were identical. One representative experiment is shown.

Fluorescence microscopy

Cultures of *B. subtilis* expressing a SalA-GFP fusion at the *salA* locus were grown at 37°C in LB, and samples were taken during the exponential growth at $OD_{600} = 0.6$. Cells were rinsed in the minimal medium and mounted on 1.2% agarose pads. Fluorescence microscopy was performed on a Leica DMR2A (100 UplanAPO objective with an aperture of 1.35. Exposure time was ≥ 5 s). System control and image processing were performed using Metamorph software (Molecular Devices, Sunnyvale, CA, USA). For each strain, foci were counted for at least 500 cells in the absence of membrane stain.

Structural modeling

Homology modeling was performed using the Swiss-Model (Arnold *et al.*, 2006), and PDBeFold server (Mary Rajathei and Selvaraj, 2013) was used for the structural superimposition.

Acknowledgements

We thank Dina Petranovic for valuable discussions and critical reading of the manuscript, Fredrik Westerlund for assistance with circular dichroism measurements and Silke Wahl and Johannes Madlung for excellent technical support. This work was supported by the Agence Nationale de la Recherche (2010-BLAN-1303-01) (to IM, MFNG and SN), and Chalmers University of Technology (to IM).

References

Abe, S., Yasumura, A., and Tanaka, T. (2009) Regulation of *Bacillus subtilis aprE* expression by *glnA* through inhibition of *scoC* and sigma(D)-dependent *degR* expression. *J Bacteriol* **191:** 3050–3058.

Arnold, K., Bordoli, L., Kopp, J., and Schwede, T. (2006) The SWISS-MODEL Workspace: a web-based environment for protein structure homology modelling. *Bioinformatics* **22:** 195–201.

de Boer, P.A., Crossley, R.E., Hand, A.R., and Rothfield, L.I. (1991) The MinD protein is a membrane ATPase required for the correct placement of the *Escherichia coli* division site. *EMBO J* **10:** 4371–4380.

Borchert, N., Dieterich, C., Krug, K., Schütz, W., Jung, S., Nordheim, A., *et al*. (2010) Proteogenomics of *Pristionchus pacificus* reveals distinct proteome structure of nematode models. *Genome Res* **20:** 837–846.

Chao, J.D., Wong, D., and Av-Gay, Y. (2014) Microbial protein-tyrosine kinases. *J Biol Chem* **289:** 9463–9472.

Dardel, F., Panvert, M., Blanquet, S., and Fayat, G. (1991) Locations of the *metG* and *mrp* genes on the physical map of *Escherichia coli*. *J Bacteriol* **173:** 3273.

Derouiche, A., Bidnenko, V., Grenha, R., Pigonneau, N., Ventroux, M., Franz-Wachtel, M., *et al*. (2013) Interaction of bacterial fatty-acid-displaced regulators with DNA is interrupted by tyrosine phosphorylation in the helix-turn-helix domain. *Nucleic Acids Res* **41:** 9371–9381.

Fabret, C., Ehrlich, S.D., and Noirot, P. (2002) A new mutation delivery system for genome-scale approaches in *Bacillus subtilis*. *Mol Microbiol* **46:** 25–36.

Gerwig, J., Kiley, T.B., Gunka, K., Stanley-Wall, N., and Stülke, J. (2014) The protein tyrosine kinases EpsB and PtkA differentially affect biofilm formation in *Bacillus subtilis*. *Microbiology* **160:** 682–691.

Grangeasse, C., Obadia, B., Mijakovic, I., Deutscher, J., Cozzone, A.J., and Doublet, P. (2003) Autophosphorylation of the *Escherichia coli* protein kinase Wzc regulates tyrosine phosphorylation of Ugd, a UDP-glucose dehydrogenase. *J Biol Chem* **278:** 39323–39329.

Grangeasse, C., Nessler, S., and Mijakovic, I. (2012) Bacterial tyrosine kinases: evolution, biological function and structural insights. *Philos Trans R Soc Lond B Biol Sci* **367:** 2640–2655.

Gustafsson, M.C., Palmer, C.N., Wolf, C.R., and von Wachenfeldt, C. (2001) Fatty-acid-displaced transcriptional repressor, a conserved regulator of cytochrome P450 102 transcription in *Bacillus* species. *Arch Microbiol* **176:** 459–464.

Hausmann, A., Aguilar Netz, D.J., Balk, J., Pierik, A.J., Mühlenhoff, U., and Lill, R. (2005) The eukaryotic P loop NTPase Nbp35: an essential component of the cytosolic and nuclear iron-sulfur protein assembly machinery. *Proc Natl Acad Sci USA* **102:** 3266–3271.

Henriques, M.X., Rodrigues, T., Carido, M., Ferreira, L., and Filipe, S.R. (2011) Synthesis of capsular polysaccharide at the division septum of *Streptococcus pneumoniae* is dependent on a bacterial tyrosine kinase. *Mol Microbiol* **82:** 515–534.

Heringa, J., and Taylor, W.R. (1997) Three-dimensional domain duplication, swapping and stealing. *Curr Opin Struct Biol* **7:** 416–421.

Inaoka, T., Wang, G., and Ochi, K. (2009) ScoC regulates bacilysin production at the transcription level in *Bacillus subtilis*. *J Bacteriol* **191:** 7367–7371.

James, P., Halladay, J., and Craig, E.A. (1996) Genomic libraries and a host strain designed for highly efficient two-hybrid selection in yeast. *Genetics* **144:** 1425–1436.

Jers, C., Pedersen, M.M., Paspaliari, D.K., Schütz, W., Johnsson, C., Soufi, B., *et al*. (2010) *Bacillus subtilis* BY-kinase PtkA controls enzyme activity and localization of its protein substrates. *Mol Microbiol* **77:** 287–299.

Kiley, T.B., and Stanley-Wall, N.R. (2010) Post-translational control of *Bacillus subtilis* biofilm formation mediated by tyrosine phosphorylation. *Mol Microbiol* **78:** 947–963.

Kimura, Y., Yamashita, S., Mori, Y., Kitajima, Y., and Takegawa, K. (2011) A *Myxococcus xanthus* bacterial tyrosine kinase, BtkA, is required for the formation of mature spores. *J Bacteriol* **193:** 5853–5857.

Kleijn, R.J., Buescher, J.M., Le Chat, L., Jules, M., Aymerich, S., and Sauer, U. (2010) Metabolic fluxes during strong carbon catabolite repression by malate in *Bacillus subtilis*. *J Biol Chem* **285:** 1587–1596.

Koch, A., Krug, K., Pengelley, S., Macek, B., and Hauf, S. (2011) Mitotic substrates of the kinase Aurora with roles in chromatin regulation identified through quantitative phosphoproteomics of fission yeast. *Sci Signal* **4:** rs6.

Kolot, M., Gorovits, R., Silberstein, N., Fichtman, B., and Yagil, E. (2008) Phosphorylation of the integrase protein of coliphage HK022. *Virology* **375:** 383–390.

Mary Rajathei, D., and Selvaraj, S. (2013) Analysis of sequence repeats of proteins in the PDB. *Comput Biol Chem* **47:** 156–166.

Mijakovic, I., Poncet, S., Boël, G., Mazé, A., Gillet, S., Jamet, E., *et al*. (2003) Transmembrane modulator-dependent bacterial tyrosine kinase activates UDP-glucose dehydrogenases. *EMBO J* **22:** 4709–4718.

Mijakovic, I., Petranovic, D., Bottini, N., Deutscher, J., and Jensen, P.R. (2005) Protein-tyrosine phosphorylation in *Bacillus subtilis*. *J Mol Microbiol Biotechnol* **9:** 189–197.

Mijakovic, I., Petranovic, D., Macek, B., Cepo, T., Mann, M., Davies, J.D., *et al*. (2006) Bacterial single-stranded DNA-binding proteins are phosphorylated on tyrosine. *Nucleic Acids Res* **34:** 1588–1596.

Minic, Z., Marie, C., Delorme, C., Faurie, J.M., Mercier, G., Ehrlich, D., and Renault, P. (2007) Control of EpsE, the phosphoglycosyltransferase initiating exopolysaccharide synthesis in *Streptococcus thermophilus*, by EpsD tyrosine kinase. *J Bacteriol* **189:** 1351–1357.

Nicolas, P., Mäder, U., Dervyn, E., Rochat, T., Leduc, A.,

Pigeonneau, N., *et al*. (2012) Condition-dependent transcriptome reveals high-level regulatory architecture in *Bacillus subtilis*. *Science* **335:** 1103–1106.
Nir-Paz, R., Eugster, M.R., Zeiman, E., Loessner, M.J., and Calendar, R. (2012) *Listeria monocytogenes* tyrosine phosphatases affect wall teichoic acid composition and phage resistance. *FEMS Microbiol Lett* **326:** 151–160.
Ogura, M., Shimane, K., Asai, K., Ogasawara, N., and Tanaka, T. (2003) Binding of response regulator DegU to the *aprE* promoter is inhibited by RapG, which is counteracted by extracellular PhrG in *Bacillus subtilis*. *Mol Microbiol* **49:** 1685–1697.
Ogura, M., Matsuzawa, A., Yoshikawa, H., and Tanaka, T. (2004) *Bacillus subtilis* SalA (YbaL) negatively regulates expression of *scoC*, which encodes the repressor for the alkaline exoprotease gene, *aprE*. *J Bacteriol* **186:** 3056–3064.
Olivares-Illana, V., Meyer, P., Bechet, E., Gueguen-Chaignon, V., Soulat, D., Lazereg-Riquier, S., *et al*. (2008) Structural basis for the regulation mechanism of the tyrosine kinase CapB from *Staphylococcus aureus*. *PLoS Biol* **6:** e143.
Petranovic, D., Michelsen, O., Zahradka, K., Silva, C., Petranovic, M., Jensen, P.R., and Mijakovic, I. (2007) *Bacillus subtilis* strain deficient for the protein-tyrosine kinase PtkA exhibits impaired DNA replication. *Mol Microbiol* **63:** 1797–1805.
Petranovic, D., Grangeasse, C., Macek, B., Abdillatef, M., Gueguen-Chaignon, V., Nessler, S., *et al*. (2009) Activation of *Bacillus subtilis* Ugd by the BY-kinase PtkA proceeds via phosphorylation of its residue tyrosine 70. *J Mol Microbiol Biotechnol* **17:** 83–89.
Preneta, R., Jarraud, S., Vincent, C., Doublet, P., Duclos, B., Etienne, J., and Cozzone, A.J. (2002) Isolation and characterization of a protein-tyrosine kinase and a phosphotyrosine-protein phosphatase from *Klebsiella pneumoniae*. *Comp Biochem Physiol B Biochem Mol Biol* **131:** 103–112.
Qi, H., Li, S., Zhao, S., Huang, D., Xia, M., and Wen, J. (2014) Model-driven redox pathway manipulation for improved isobutanol production in *Bacillus subtilis* complemented with experimental validation and metabolic profiling analysis. *PLoS ONE* **9:** e93815.
Rydén, L.G., and Hunt, L.T. (1993) Evolution of protein complexity: the blue copper-containing oxidases and related proteins. *J Mol Evol* **36:** 41–66.
Seeliger, D., and de Groot, B.L. (2010) Ligand docking and binding site analysis with PyMOL and Autodock/Vina. *J Comput Aided Mol Des* **24:** 417–422.
Shapland, E.B., Reisinger, S.J., Bajwa, A.K., and Ryan, K.R. (2011) An essential tyrosine phosphatase homolog regulates cell separation, outer membrane integrity, and morphology in *Caulobacter crescentus*. *J Bacteriol* **193:** 4361–4370.
Shi, L., Kobir, A., Jers, C., and Mijakovic, I. (2010) Bacterial protein-tyrosine kinases. *Curr Proteomics* **7:** 188–194.
Shi, L., Ji, B., Kolar-Znika, L., Boskovic, A., Jadeau, F., Combet, C., *et al*. (2014a) Evolution of bacterial protein-tyrosine kinases and their relaxed specificity towards substrates. *Genome Biol Evol* **6:** 800–817.
Shi, L., Pigeonneau, N., Ventroux, M., Derouiche, A., Bidnenko, V., Mijakovic, I., and Noirot-Gros, M.F. (2014b) Protein-tyrosine phosphorylation interaction network in *Bacillus subtilis* reveals new substrates, kinase activators and kinase cross-talk. *Front Microbiol* **5:** 538.
Soulat, D., Jault, J.M., Duclos, B., Geourjon, C., Cozzone, A.J., and Grangeasse, C. (2006) *Staphylococcus aureus* operates protein-tyrosine phosphorylation through a specific mechanism. *J Biol Chem* **281:** 14048–14056.
Van Damme, E.J., Nakamura-Tsuruta, S., Smith, D.F., Ongenaert, M., Winter, H.C., Rougé, P., *et al*. (2007) Phylogenetic and specificity studies of two-domain GNA-related lectins: generation of multispecificity through domain duplication and divergent evolution. *Biochem J* **404:** 51–61.
Vitale, G., Fabre, E., and Hurt, E.C. (1996) NBP35 encodes an essential and evolutionary conserved protein in Saccharomyces cerevisiae with homology to a superfamily of bacterial ATPases. *Gene* **178:** 97–106.
Vogel, C., and Morea, V. (2006) Duplication, divergence and formation of novel protein topologies. *Bioessays* **28:** 973–978.
Vogel, C., Teichmann, S.A., and Pereira-Leal, J. (2005) The relationship between domain duplication and recombination. *J Mol Biol* **346:** 355–365.
Walker, J.E., Saraste, M., Runswick, M.J., and Gay, N.J. (1982) Distantly related sequences in the alpha- and beta-subunits of ATP synthase, myosin, kinases and other ATP-requiring enzymes and a common nucleotide binding fold. *EMBO J* **1:** 945–951.

Supporting information

Additional supporting information may be found in the online version of this article at the publisher's web-site.